INORGANIC CHEMISTRY
FRONTIERS

RESEARCH ARTICLE

View Article Online
View Journal | View Issue

Cite this: *Inorg. Chem. Front.*, 2022, **9**, 1777

Redox-active hierarchical assemblies of hybrid polyoxometalate nanostructures at carbon surfaces†

Sharad S. Amin,[a] Jamie M. Cameron, *[a] Richard B. Cousins,[b] James Wrigley,[c] Letizia Liirò-Peluso,[a,c] Victor Sans, [d] Darren A. Walsh *[a] and Graham N. Newton *[a]

Received 20th January 2022,
Accepted 2nd March 2022

DOI: 10.1039/d2qi00174h

rsc.li/frontiers-inorganic

The self-assembly of hierarchical nanostructures on surfaces is a promising strategy for the development of a wide range of new technologies, such as energy-storage devices and sensors. In this work we show that amphiphilic, organofunctionalized hybrid polyoxometalates spontaneously self-assemble on glassy carbon, graphene oxide, and highly oriented pyrolytic graphite to create hierarchical redox-active nanostructures. The electrochemical behaviour and stability of these supramolecular, nanostructured assemblies is explored in detail and their morphology is determined by comprehensive optical and spectroscopic analyses. The spontaneous assembly of these hybrid nanomaterials on both hydrophilic and hydrophobic carbons is compared and we discuss how this strategy may be a new, simple, and effective method of fabricating hierarchically modified electrode surfaces.

Introduction

The development of chemically modified electrodes is one of the most significant advances in the field of electrochemistry in the past 30 years.[1] Modification of electrode surfaces with functional molecules and materials has led to breakthroughs in the fields of sensing,[2] energy storage,[3] catalysis,[4] photonics,[5] genomics,[6] and memory storage.[7,8] The self-assembly of molecular components onto an electrode surface to form well-defined adsorbate layers can be a particularly cost-effective and simple route to the development of functional electronic devices.[9] A very well-known example is the attachment of molecules to gold electrodes *via* thiol groups; an approach that can be readily used to develop systems for fundamental studies into electron transfer dynamics at the nanoscale,[10] and forms the basis for a range of electronic devices.[9] In contrast to other electrode modification strategies, the "bottom-up" self-assembly of molecular components can yield extremely well-defined complex surfaces, often without the need for advanced synthetic skills or technical know-how.

Recently, polyoxometalates (POMs), a class of polyanionic molecular metal oxide clusters constructed from early transition metals in their highest oxidation states (*e.g.* W^{VI}, Mo^{VI} and V^{V}), have emerged as excellent building blocks for the preparation of self-assembled redox-active nanostructures.[11] POMs exhibit a range of attractive properties, including highly reversible multi-redox behaviour, rich acid/base chemistry, and wide-ranging and tuneable physicochemical properties due to their extraordinary range of possible structures and compositions.[12–14] POMs can also be selectively functionalised through the covalent attachment of organic groups, yielding new species commonly referred to as organic–inorganic hybrid POMs.[15–17] The tuneability of the organic moieties means that these systems can be specifically functionalised to target certain surfaces and/or interaction types. For example, recent studies by Proust and co-workers reported examples of thiol or diazonium-modified hybrid POMs binding to gold and silicon surfaces through covalent interactions.[18,19] Similarly, the deposition of POMs onto electrode materials has been achieved through non-covalent strategies including electrostatic interactions,[20] π–π interactions,[21] and oxidation of electrode surfaces to promote weak interactions.[22] A particular advantage offered by hybrid POMs is their capacity to act as amphiphiles and form ordered superstructures such as micelles and

[a]*GSK Carbon Neutral Laboratory, University of Nottingham, Nottingham, NG8 2TU, UK. E-mail: jamie.cameron1@nottingham.ac.uk, darren.walsh@nottingham.ac.uk, graham.newton@nottingham.ac.uk*
[b]*Nanoscale and Microscale Research Centre, University of Nottingham, Nottingham, NG7 2RD, UK*
[c]*School of Physics and Astronomy, University of Nottingham, Nottingham NG7 2RD, UK*
[d]*Institute of Advanced Materials, Universitat Jaume I, 12006 Castello, Spain*

†Electronic supplementary information (ESI) available: Full experimental details and additional cyclic voltammetry, dynamic light scattering, atomic force microscopy, scanning electron microscopy and ellipsometry measurements. See DOI: 10.1039/d2qi00174h

vesicles in solution.[23–25] Recent work in our group has demonstrated that the redox properties of molecular hybrid POMs are translated to solution-phase supramolecular assemblies.[23,25] Subsequently, this work has been expanded on by Polarz and co-workers, who explored the redox chemistry of hybrid micellar assemblies, proposing that such systems may have significant implications in energy storage technologies.[24]

Here we set out to develop our understanding of the redox properties of supramolecular POM assemblies by moving out of the solution phase and focussing on the self-assembly of hybrid POM nanostructures on electrode surfaces. We hypothesised that amphiphilic hybrid POMs would interact differently with different carbon surfaces and that the weak interactions between the POMs and the surfaces would be sufficient to stabilise a range of hybrid materials. We show that micellar aqueous solutions of hybrid POMs form nanostructured monolayer assemblies when adsorbed onto (relatively) hydrophilic carbons (graphene oxide (GO) and glassy carbon (GC)), and that they spontaneously reassemble to yield complex lamellar assemblies on hydrophobic carbon (highly ordered pyrolytic graphite (HOPG)). The redox properties of the glassy-carbon-adsorbed material are found to be consistent with those of solution-phase POM assemblies. To the best of our knowledge, this paper constitutes the first study into the fundamental interactions of amphiphilic POMs with different carbon surfaces, which can give rise to opportunities in fabrication of functional nanostructured surfaces.

Results and discussion

Preparation of self-assembled monolayers

Condensation of (4-(icosyloxy)phenyl)phosphonic acid ($C_{20}H_{41}OC_6H_4PO_3H_2$) and the lacunary Wells–Dawson cluster $K_{10}[P_2W_{17}O_{61}]$ yielded the hybrid-POM species $K_6[P_2W_{17}O_{61}(P(O)C_6H_4OC_{20}H_{41})_2]$ ($\{W_{17}C_{20}\}$), in agreement with our previously-reported method.[23] Due to its properties as an anionic surfactant (combining a polar POM head-group and non-polar long-chain alkane tails), $\{W_{17}C_{20}\}$ spontaneously assembles in aqueous solutions to form micellar structures with hydrodynamic diameters in the range of 5–7 nm. These supramolecular assemblies display different redox behaviours when compared to the molecular species (which can be stabilised by the addition of polar organic solvents, such as dimethylformamide (DMF)).[23,25] Specifically, we previously observed that the redox behaviour of the micelles was consistent with being surface-bound at the glassy carbon electrode and strongly dependent on the amphiphile chain length, where shorter-chain species (*e.g.* $\{W_{17}C_{10}\}$) tend towards solution-state/diffusion-controlled electrochemical properties.[23] This suggested that the more stable supramolecular nanostructures formed by $\{W_{17}C_{20}\}$ interact strongly with the surface of the carbon electrode and form a new, robust and electrochemically distinct interface (Fig. 1).

Building on this observation, we set out here to investigate the hierarchical self-assembly of the $\{W_{17}C_{20}\}$ anionic surfactant across a range of carbon surfaces in order to better understand the self-assembly processes of the hybrid-POM on these common electrode materials. In particular, we were interested in the effect of surface hydrophilicity on the assembly/deposition of the supramolecular structures onto the carbon surfaces from the solution phase. In general, modified carbon surfaces were prepared using aqueous, micellar solutions of the $\{W_{17}C_{20}\}$ hybrid-POM in one of two ways. For glassy carbon (GC), a standard 3 mm GC electrode was dipped into a 1.4 mM solution of $\{W_{17}C_{20}\}$ in 0.1 M H_2SO_4 for 1 min (without stirring), removed and rinsed with deionised water, and then allowed to air dry. Preparation of modified graphene oxide (GO) and highly ordered pyrolytic graphite (HOPG) surfaces for comparison with GC was performed by drop-casting either 1.4 mM aqueous or acidic (0.1 M H_2SO_4) solutions of $\{W_{17}C_{20}\}$ micelles directly onto the relevant material, blotting to remove excess solution and then air-drying.

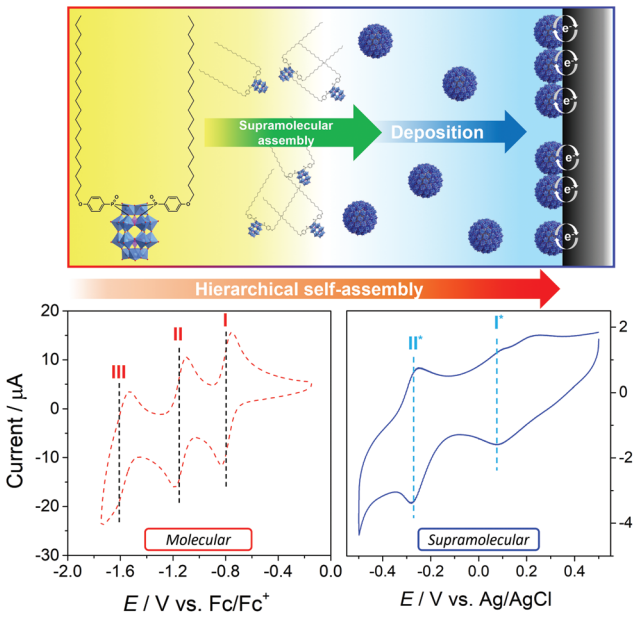

Fig. 1 A schematic illustrating the hierarchical supramolecular assembly of redox-active $\{W_{17}C_{20}\}$ in aqueous solutions onto glassy carbon, and CV plots of (red) 1.4 mM $\{W_{17}C_{20}\}$ in DMF (*i.e.* the molecular system) with 0.1 M [TBA][PF_6], and; (blue) 1.4 mM $\{W_{17}C_{20}\}$ in 0.1 M H_2SO_4 (*i.e.* the surface-bound system).

Electrochemical analysis

As described above, we have previously reported that the redox behaviour of the molecular and micellar forms of $\{W_{17}C_{20}\}$ differ and that, furthermore, this property is switchable by way of the solvent used. Under aqueous conditions, $\{W_{17}C_{20}\}$ spontaneously assembles into micelles (as confirmed by dynamic light scattering (DLS) analysis of the solution) but, on addition of a polar organic solvent, the micelles rapidly disassemble to give a solution of discrete $\{W_{17}C_{20}\}$ clusters.

Cyclic voltammetry (CV) of a 1.4 mM solution of $\{W_{17}C_{20}\}$ micelles in 0.1 M H_2SO_4 using a glassy carbon working elec-

trode produces a voltammogram showing two pseudo-reversible redox waves: an ill-defined process at $E_{1/2}$ = 0.089 V *vs.* Ag^+/Ag (I*) and a well-defined, highly reversible wave at more negative potential $E_{1/2}$ = −0.265 V (II*) (Fig. 1), both of which are ascribed to 2-electron redox processes based on comparison to a previously reported, analogous system.[25] DMF was then added directly to the electrochemical cell (to give a 50 : 50 v/v solution) and the CV was then remeasured. This gives a voltammogram corresponding directly to the solvated molecular species (Fig. S2†), clearly indicating the spontaneous transformation of the micelles back into the molecular hybrid-POM precursor. Here, three pseudo-reversible redox waves are observed at $E_{1/2}$ = 0.070 V (I), −0.027 V (II) and −0.353 V (III), with processes I and II being single electron transfers and process III remaining a 2-electron process. Taking into account the moderate overall negative shift in redox potentials expected due to the addition of a lower polarity solvent like DMF,[23] the key difference between both species corresponds to the coalescence of peaks I and II into a single process (peak I*) when the hybrid-POM is assembled into micelles. We attribute this to increased coulombic repulsion between adjacent POM head-groups in the tightly-packed micelle shells causing the LUMO level of **{$W_{17}C_{20}$}** (*i.e.* corresponding to process I) to increase substantially in energy, causing an additional negative shift in redox potential so as to overlap with process II.[23,25]

Further to the differing redox profiles of each species, we were also able to make several observations which suggest that each system is also behaving differently in relation to the electrode surface itself. For instance, the peak-to-peak separation (ΔE_p) observed in the micellar system is significantly smaller than in the molecular voltammetry (*e.g.* process II* = 29 mV *vs.* 207 mV for the equivalent 2e process III). Furthermore, a plot of peak current (I_p) measured against various scan rates displays a linear trend, which is clear evidence of a surface-confined electrochemical response (Fig. S4†). Taken together, this supports our hypothesis that **{$W_{17}C_{20}$}** micelles adsorb onto the surface of the GC electrode, while the hybrid-POM in its molecular form remains freely diffusing in solution.

Surface adsorption of **{$W_{17}C_{20}$}** to the GC surface was unambiguously confirmed by dip-testing. A freshly polished GC electrode was dipped in a 1.4 mM solution of **{$W_{17}C_{20}$}** in 0.1 M H_2SO_4 for 1 min, before removing and rinsing thoroughly with deionised water. The same electrode was then placed in fresh 0.1 M H_2SO_4 electrolyte and a series of voltammetric sweeps performed using identical conditions to those in the experiments described above. A near-identical voltammogram to that reported in Fig. 1 was observed on the first cycle and the redox properties remained stable over a series of 100 full potential sweeps (Fig. 2). An identical dip test using an aqueous solution of **{$W_{17}C_{20}$}** without the supporting H_2SO_4 electrolyte led to no detectable deposition of the hybrid POM. This method confirms both that: (a) the micellar species spontaneously and rapidly adhere to the GC surface in the presence of acid, and; (b) the micelles are not electrodeposited but rather, chemically adsorbed to the surface. The importance of acid in the deposition process suggests that H_2SO_4 is either promoting surface

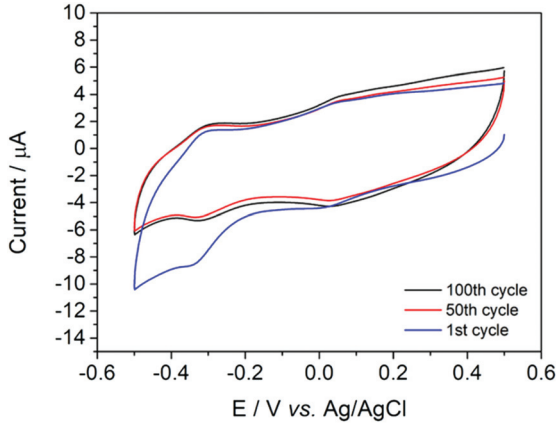

Fig. 2 A cyclic voltammogram of **{$W_{17}C_{20}$}** taken after deposition on a GC electrode, rinsing and then measured in fresh 0.1 M H_2SO_4 electrolyte, displaying cycles 1 (blue), 50 (red) and 100 (black).

oxidation of the carbon in order to produce functional groups which facilitate favourable non-covalent interactions between **{$W_{17}C_{20}$}** and the GC surface (a phenomenon recently observed in POM-activated carbon composites),[22] or that the protons otherwise act as bridging agents between the carbon and metal–oxide surfaces to facilitate deposition. We discuss these hypotheses in more detail below.

Once the deposition mechanism and stability of the material was understood, we set out to estimate the number of redox-active micelles at the electrode surface. If we assume the approximate surface area of the electrode (d = 3 mm) is 7.07 × 10^{-6} m^2 and the micelle (D_h = 7 nm, 61 POM clusters, each with cross-sectional area of 2.5 × 10^{-18} m^2 per micelle) average cross-sectional area is 3.85 × 10^{-17} m^2, then the approximate number of micelles in a full monolayer would be 1.84 × 10^{11} micelles (1.86 × 10^{-11} mol of POM). From reduction process II (100^{th} cycle), which we know to be a $2e^-$ process, the charge passed (Q = 9.3 × 10^{-7} C) was acquired by integrating the area under the curve and was used to calculate the number of moles of POMs (8 × 10^{-12}) involved in the reduction process using the equation $Q = nFM$, (where n = no. of electrons transferred per molecule, F = Faraday constant (96 500 C mol^{-1}) and M = no. of moles of species reacting). This calculation concluded that in a theoretical full monolayer of micelles on a flat GC surface, 43% of the POMs in a micelle were involved in the redox process (see ESI† for full details). This value suggests that, either: the full monolayer (i.e. ~100% surface coverage) is not fully redox active/accessible, which could be attributed to slow electron transfer kinetics around the micelle, or; the deposited micelles do not form a full monolayer. Surface characterisation provided below suggests that the former is the more likely.

Surface characterisation of modified glassy carbon electrodes

Following unambiguous confirmation of the deposition and stability of a new surface-bound POM-based interface from micellar solutions of **{$W_{17}C_{20}$}**, we next explored a range of

surface characterisation techniques to identify the morphology of the deposited material. The surface structure of the electrode was first analysed using imaging ellipsometry. Fig. 3c displays the ellipsometry surface mapping of the modified GC electrode where we observed a layer of deposited material with a thickness of 6–8 nm. This corroborates well with the hydrodynamic diameter of the $\{W_{17}C_{20}\}$ micelles observed through DLS analysis (Fig. S6†) and strengthens the argument that the micelles form a self-assembled monolayer on the GC surface. Intermittent contact-mode Atomic force microscopy (AC-mode AFM), using a Scout 70R cantilever (Nunano), was performed under ambient conditions to analyse the modified electrode at nanometre resolution and confirmed the presence of spherical structures on the carbon surface with diameters ranging between 5–30 nm. Additional height profile analysis of the spherical objects (Fig. 3a) gives an average height of 6 nm and width of 19.2 nm, again corresponding well to the known solution-phase dimensions of the micelles. The additional width of the surface-bound nanostructures could be a result of agglomeration or flattening upon deposition on the surface. The corresponding phase image (Fig. S8†) also shows clear spherical structures with sizes between 5–15 nm. Additional scanning electron microscopy (SEM) further confirmed both high coverage of the deposited material and its overall morphology (Fig. 3d), showing a largely uniform deposit of what look to be very fine particles on the amorphous carbon surface. Taken together, it is clear from these analyses that we can prepare a stable redox-active monolayer of micelles at the surface of GC electrodes which are held through electrostatic interactions between the POM and carbon surface functionality (*e.g.* carboxylic acids) introduced by potential acid catalysed surface oxidation.[23] To the best of our knowledge, our result represents the first example of redox-active hybrid-POM monolayers (ML) or SAM consisting of electrostatically bound hybrid-POM micelles.

Surface-controlled self-assembly

Following our analysis of the redox-active self-assembled monolayers we observe on glassy carbon, we were interested to explore how the type and properties of the surface affect the deposition and hierarchical assembly of the $\{W_{17}C_{20}\}$ surfactant. To deepen our understanding of the key factors involved in the deposition and assembly of the hybrid-POM micelles, we drop cast 1.4 mM aqueous solutions of $\{W_{17}C_{20}\}$ on both (relatively) hydrophilic graphene oxide (GO) (Fig. 4) and hydrophobic highly oriented pyrolytic graphite (HOPG) (Fig. 5) as a point of comparison. On GO, transmission electron microscopy (TEM) analysis shows that $\{W_{17}C_{20}\}$ deposits on the surface as a close packed monolayer of micelles (Fig. 4b) with very low polydispersity and diameters ranging from

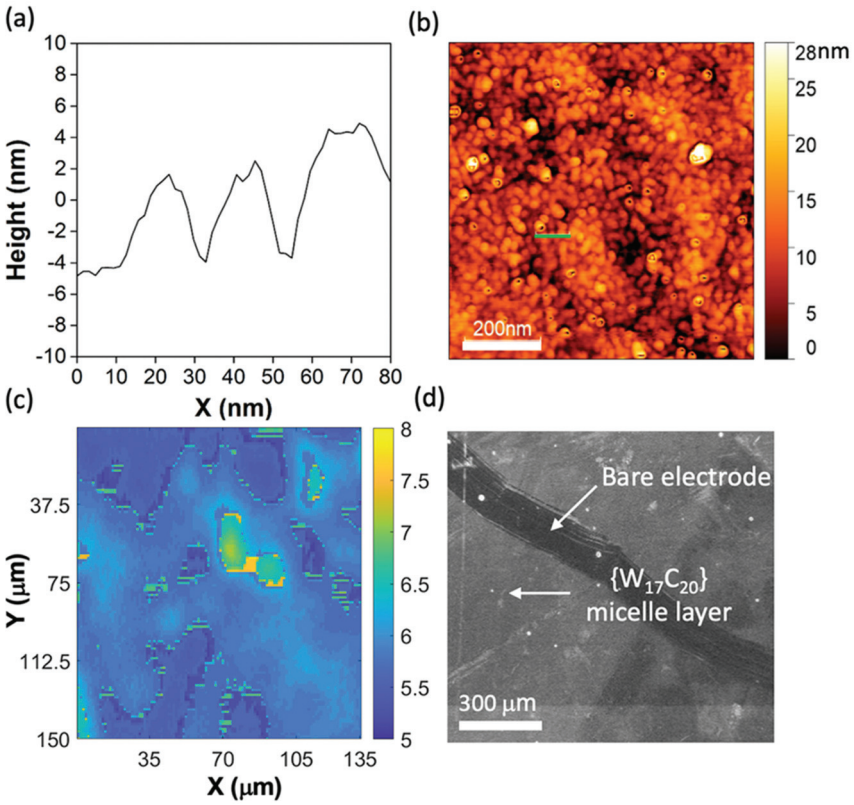

Fig. 3 (a) $\{W_{17}C_{20}\}$@GC electrode height trace plot of section highlighted (green) in panel b, (peak full width half maxima = 12.1 nm); (b) AFM plot of $\{W_{17}C_{20}\}$@GC electrode; (c) ellipsometry map of the prepared GC square electrode post CV, displaying regions of deposition from 5–8 nm thickness; (d) SEM image displaying areas of deposition (light grey) and an area of bare electrode that has been (inadvertently) mechanically abraded (dark grey).

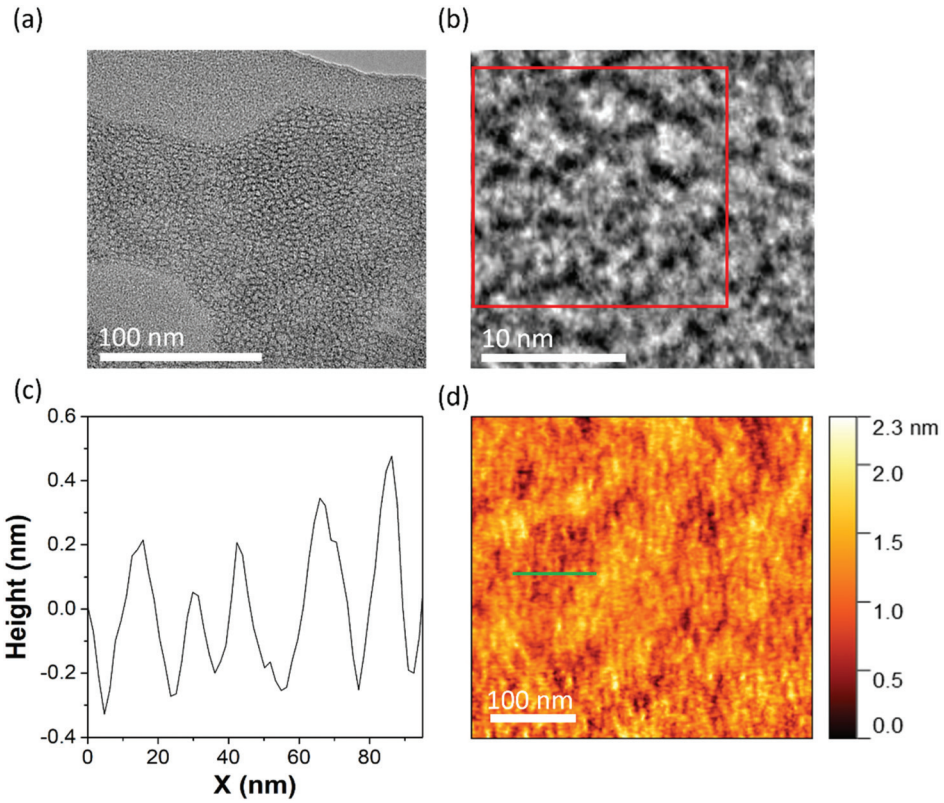

Fig. 4 (a) TEM image of micelle packing nanopattern assembled by drop casting 1.4 mM $\{W_{17}C_{20}\}$ onto a GO TEM grid; (b) high magnification image, highlighting the packing of the micelles on GO (focused in red box); (c) height trace plot from the area highlighted by the green line in panel d (peak half width full maxima = 5.5 nm), and; (d) atomic force microscopic surface analysis of the micelle packing on a GO TEM grid.

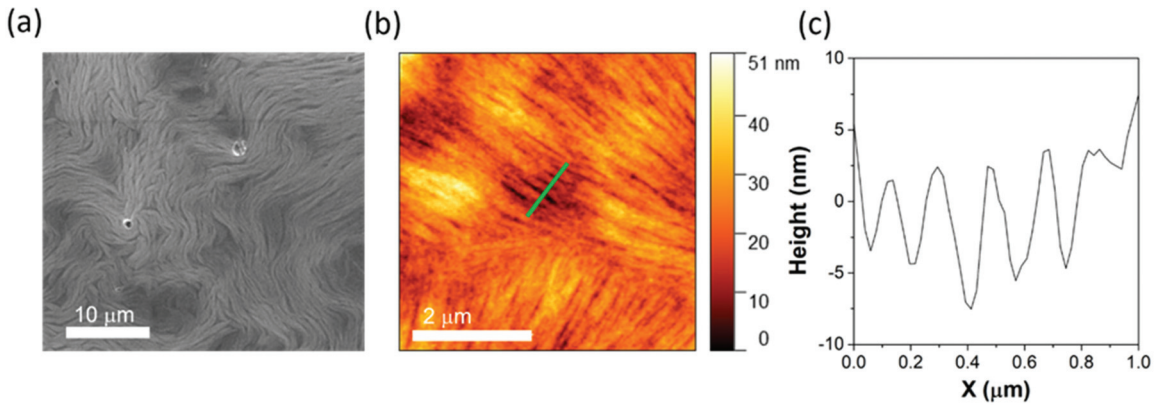

Fig. 5 (a) SEM image of $\{W_{17}C_{20}\}$ drop casted onto hydrophobic HOPG; (b) atomic force microscopy plot of $\{W_{17}C_{20}\}$@HOPG, and; (c) height trace plot of section highlighted (green) in panel b displaying lamellar structures approximately 8 nm in height (half width full maxima = 70 nm).

6–9 nm, in excellent agreement with the hydrodynamic diameter of the micelles measured by DLS (Fig. S6†). The close-packed arrangement is particularly interesting and not what might be usually expected based on the highly-charged surface of the micelles, which might normally lead to high electrostatic repulsion between neighbouring structures (each POM head-group carries a formal charge of 6-). Here, this observation is most likely a result of cation intercalation between the charged micelles and macroions, which has been discussed in depth by the likes of Liu *et al.*[26,27] AFM analysis further supports identification of a close-packed layer of micellar structures (Fig. 4d), where a roughness plot of the surface shows structures with an average diameter of 7 nm, again corresponding strongly to the micelles known dimensions. Unlike deposition on GC however, height analysis of the surface does not correlate with the diameter of the micelles

which we attribute to the efficient close packing of the micelles (where the AFM tip is actually measuring the shallow 'groove' of *ca.* 0.5 nm between adjacent structures (Fig. 4c).

We also note that this observation is also in good agreement with our results described above for GC and supports our hypothesis that the presence of acid is critical in order to 'activate' the GC surface (without which, no deposition occurs).[28] The GO surface is significantly more hydrophilic than typical carbon materials due to its surface oxidation,[29] which makes the interaction between the highly polar, strongly hydrogen-bonding metal–oxide surface of the micelles and the polar functional groups (*e.g.* epoxides, alcohols, and carboxylic acids *etc.*) on the GO surface dominant, favouring retention of the micelle structure rather than rearrangement on the carbon surface. Note that the same close-packed morphology was observed by TEM when $\{W_{17}C_{20}\}$ was drop cast onto GO from 0.1 M H_2SO_4 solutions rather than water alone (Fig. S9†). This would strongly suggest the fundamental surface chemistry of the carbon itself is the dominant influence on the hierarchical surface-assembly of the hybrid-POM, rather than the protons acting as a mediator between the carbon and the supramolecular hybrid-POM nanostructures.

This idea is further supported by analysis of the morphology of $\{W_{17}C_{20}\}$ when drop cast from water onto HOPG. Here, the carbon surface is much more hydrophobic, removing any possibility for favourable interactions between the carbon and the outer surface of the micelle. SEM analysis of the modified HOPG shows much larger and clearly lamellar fibrous nanostructures (Fig. 5a), demonstrating a spontaneous rearrangement of the hydrophilic $\{W_{17}C_{20}\}$ micelles once they encounter the hydrophobic HOPG surface.[30,31] AFM further supports the formation of large fibrous nanostructures (Fig. 5b), and analysis of the surface roughness plot indicates that the lamellar fibres are between 100–400 nm in width and between 20–30 nm in height (Fig. 5c). The spontaneous rearrangement of $\{W_{17}C_{20}\}$ on HOPG is evidence that the hydrophobic effect responsible for assembly of the micelles in aqueous solutions clearly superseded by the interaction between the long-chain C_{20}-groups on the hybrid-POM cluster and the non-polar carbon surface.

As an example of this, several groups have previously observed the formation of similar nanofiber and tubular assemblies on HOPG through deposition of long-chain or branched cationic surfactants.[30,31] Bai *et al.* reported that hexadecyltrimethylammonium bromide deposits horizontally on HOPG with the ionic head-groups aligned head-to-head and the alkane chain lying parallel to the carbon surface, where the interaction between the carbon chains and graphite surface in the wetting stage of the deposition process determines the supramolecular organisation. A similar mechanism can be proposed for $\{W_{17}C_{20}\}$ due to its broad chemical similarity (a highly polar ionic head-group with long-chain alkane tails), which would suggest the formation of lamellar sheets of the hybrid-POM amphiphile around 16–24 clusters thick based on the AFM analysis described above. Interestingly, when deposited from acidic solution, $\{W_{17}C_{20}\}$ forms a similar lamellar nanofibrous structure on the surface of the HOPG, however a slight difference in the overall morphology is observed *via* SEM analysis (Fig. S10†). In this instance, although nanofibres of similar width and thickness are formed (as expected based on the dominant surface interactions between the HOPG and $\{W_{17}C_{20}\}$), formation of a more sponge-like microporous network structure is apparent in the presence of acid.

Conclusions

We have described a new strategy to prepare self-assembled, multi-redox active metal oxide nanostructures on a range of common carbon electrode surfaces. This approach exploits the spontaneous self-assembly of an amphiphilic organofunctionalised polyoxometalate cluster, $\{W_{17}C_{20}\}$, which forms small, relatively monodisperse micelles in aqueous media. Using detailed surface characterisation techniques, we show that these micelles spontaneously deposit on carbon to form a range of different soft nanostructures in response to the relative hydrophilicity of the carbon surface. On both glassy carbon (though only when acid is present) and graphene oxide, the micelles deposit as a close-packed monolayer whereas on hydrophobic HOPG, the micelles re-assemble to form a multi-layer lamellar structure. Detailed electrochemical characterisation of $\{W_{17}C_{20}\}$@GC shows that the multi-redox properties of the POM 'building blocks' are retained and that the modified electrode surface is robust and stable to up to at least 100 potential sweeps when measured in fresh electrolyte solution. Our results point to a new, straightforward strategy to modify surfaces with new, highly nanostructured functional assemblies of significant interest in the development of new functional surfaces for electrocatalytic or sensing applications.

Conflicts of interest

There are no competing interests to declare.

Acknowledgements

The authors gratefully acknowledge the support of the EPSRC through the Centre for Doctoral Training in Sustainable Chemistry (EP/L015633/1) and the Nottingham Propulsion Futures Beacon of Excellence. GNN and JMC thank the Leverhulme Trust (RPG-2016-442). SSA thanks the EPSRC for the award of a Doctoral Prize.

References

1 G. A. Edwards, A. J. Bergren and M. D. Porter, Chemically Modified Electrodes in *Handbook of Electrochemistry*, ed. C. G. Zoski, Elsevier, Amsterdam, 2007, ch. 8, pp. 295–327.

2 P. Pinyou, V. Blay, L. M. Muresan and T. Noguer, Enzyme-modified electrodes for biosensors and biofuel cells, *Mater. Horiz.*, 2019, **6**, 1336–1358.
3 J. S. Wei, T. B. Song, P. Zhang, X. Q. Niu, X. B. Chen and H.-M. Xiong, A new generation of energy storage electrode materials constructed from carbon dots, *Mater. Chem. Front.*, 2020, **4**, 729–749.
4 Y. C. Hsieh, L. E. Betancourt, S. D. Senanayake, E. Hu, Y. Zhang, W. Xu and D. E. Polyansky, Modification of CO_2 Reduction Activity of Nanostructured Silver Electrocatalysts by Surface Halide Anions, *ACS Appl. Energy Mater.*, 2019, **2**, 102–109.
5 L. M. Otto, E. A. Gaulding, C. T. Chen, T. R. Kuykendall, A. T. Hammack, F. M. Toma, D. F. Ogletree, S. Aloni, B. J. H. Stadler and A. M. Schwartzberg, Methods for tuning plasmonic and photonic optical resonances in high surface area porous electrodes, *Sci. Rep.*, 2021, **11**, 7656.
6 J. D. Slinker, N. B. Muren, A. A. Gorodetsky and J. K. Barton, Multiplexed DNA-Modified Electrodes, *J. Am. Chem. Soc.*, 2010, **132**, 2769–2774.
7 A. Vilan, D. Aswal and D. Cahen, Large-Area, Ensemble Molecular Electronics: Motivation and Challenges, *Chem. Rev.*, 2017, **117**, 4248–4286.
8 A. Vilan and D. Cahen, Chemical Modification of Semiconductor Surfaces for Molecular Electronics, *Chem. Rev.*, 2017, **117**, 4624–4666.
9 S. Casalini, C. A. Bortolotti, F. Leonardi and F. Biscarini, Self-assembled monolayers in organic electronics, *Chem. Soc. Rev.*, 2017, **46**, 40–71.
10 H. O. Finklea and D. D. Hanshew, Electron-transfer kinetics in organized thiol monolayers with attached pentaammine(pyridine)ruthenium redox centers, *J. Am. Chem. Soc.*, 1992, **114**, 3173–3181.
11 S. Landsmann, C. Lizandara-Pueyo and S. Polarz, A new class of surfactants with multinuclear, inorganic head groups, *J. Am. Chem. Soc.*, 2010, **132**, 5315–5321.
12 J. M. Cameron, D. J. Wales and G. N. Newton, Shining a light on the photo-sensitisation of organic–inorganic hybrid polyoxometalates, *Dalton Trans.*, 2018, **47**, 5120–5136.
13 D.-L. Long, R. Tsunashima and L. Cronin, Polyoxometalates: Building Blocks for Functional Nanoscale Systems, *Angew. Chem., Int. Ed.*, 2010, **49**, 1736–1758.
14 N. I. Gumerova and A. Rompel, Synthesis, structures and applications of electron-rich polyoxometalates, *Nat. Rev. Chem.*, 2018, **2**, 0112.
15 A. Dolbecq, E. Dumas, C. R. Mayer and P. Mialane, Hybrid Organic–Inorganic Polyoxometalate Compounds: From Structural Diversity to Applications, *Chem. Rev.*, 2010, **110**, 6009–6048.
16 A. V. Anyushin, A. Kondinski and T. N. Parac-Vogt, Hybrid polyoxometalates as post-functionalization platforms: from fundamentals to emerging applications, *Chem. Soc. Rev.*, 2020, **49**, 382–432.
17 A. J. Kibler and G. N. Newton, Tuning the electronic structure of organic–inorganic hybrid polyoxometalates: The crucial role of the covalent linkage, *Polyhedron*, 2018, **154**, 1–20.
18 Q. Zhu, B. Paci, A. Generosi, S. Renaudineau, P. Gouzerh, X. Liang, C. Mathieu, C. Rountree, G. Izzet, A. Proust, N. Barrett and L. Tortech, Conductivity via Thermally Induced Gap States in a Polyoxometalate Thin Layer, *J. Phys. Chem. C*, 2019, **123**(3), 1922–1930.
19 S. Gam Derouich, C. Rinfray, G. Izzet, J. Pinson, J.-J. Gallet, F. Kanoufi, A. Proust and C. Combellas, Control of the Grafting of Hybrid Polyoxometalates on Metal and Carbon Surfaces: Toward Submonolayers, *Langmuir*, 2014, **30**, 2287–2296.
20 S. M. Lauinger, B. D. Piercy, W. Li, Q. Yin, D. L. Collins-Wildman, E. N. Glass, M. D. Losego, D. Wang, Y. V. Geletii and C. L. Hill, Stabilization of Polyoxometalate Water Oxidation Catalysts on Hematite by Atomic Layer Deposition, *ACS Appl. Mater. Interfaces*, 2017, **9**, 35048–35056.
21 L. Huang, J. Hu, Y. Ji, C. Streb and Y.-F. Song, Pyrene-Anderson-Modified CNTs as Anode Materials for Lithium-Ion Batteries, *Chem. – Eur. J.*, 2015, **21**, 18799–18804.
22 N. S. Mughal, D. A. Walsh and G. N. Newton, Functionalization of Carbon Surfaces Tunes the Redox Stability of Polyoxometalate@Carbon Electrodes, *ACS Appl. Energy Mater.*, 2020, **3**, 12308–12315.
23 S. Amin, J. M. Cameron, J. A. Watts, D. A. Walsh, V. Sans and G. N. Newton, Effects of chain length on the size, stability, and electronic structure of redox-active organic–inorganic hybrid polyoxometalate micelles, *Mol. Syst. Des. Eng.*, 2019, **4**, 995–999.
24 A. Klaiber, T. Kollek, S. Cardinal, N. Hug, M. Drechsler and S. Polarz, Electron Transfer in Self-Assembled Micelles Built by Conductive Polyoxometalate-Surfactants Showing Battery-Like Behavior, *Adv. Mater. Interfaces*, 2018, **5**, 1701430.
25 K. Kastner, A. J. Kibler, E. Karjalainen, J. A. Fernandes, V. Sans and G. N. Newton, Redox-active organic-inorganic hybrid polyoxometalate micelles, *J. Mater. Chem. A*, 2017, **5**, 11577–11581.
26 Z. Liu, T. Liu and M. Tsige, Elucidating the Origin of the Attractive Force among Hydrophilic Macroions, *Sci. Rep.*, 2016, **6**, 26595.
27 Z. Liu, T. Liu and M. Tsige, Unique Symmetry-Breaking Phenomenon during the Self-assembly of Macroions Elucidated by Simulation, *Sci. Rep.*, 2018, **8**, 13076.
28 H. Gunasingham and B. Fleet, Effect of pH on the response of glassy carbon electrodes, *Analyst*, 1983, **108**, 316–321.
29 I. Khosravi, Z. Shahryari, S. M. J. Moghadas, H. T. Sarraf and M. Yeganeh, *The application of graphene oxide as corrosion barrier in Corrosion Protection at the Nanoscale*, ed. S. Rajendran, T. A. N. H. Nguyen, S. Kakooei, M. Yeganeh and Y. Li, Elsevier, 2020, ch. 8, pp. 127–140.
30 S.-L. Xu, C. Wang, Q.-D. Zeng, P. Wu, Z.-G. Wang, H.-K. Yan and C.-L. Bai, Self-Assembly of Cationic Surfactants on a

Graphite Surface Studied by STM, *Langmuir*, 2002, **18**, 657–660.

31 H. Kawasaki, M. Uota, T. Yoshimura, D. Fujikawa, G. Sakai, R. Arakawa and T. Kijima, Self-Organization of Surfactant–Metal-Ion Complex Nanofibers on Graphite Surfaces and Their Application to Fibrously Concentrated Platinum Nanoparticle Formation, *Langmuir*, 2007, **23**, 11540–11545.